

Role of Metals in the Reaction Catalyzed by Protein Farnesyltransferase[†]Matthew J. Saderholm,[‡] Kendra E. Hightower,[§] and Carol A. Fierke^{*,||}

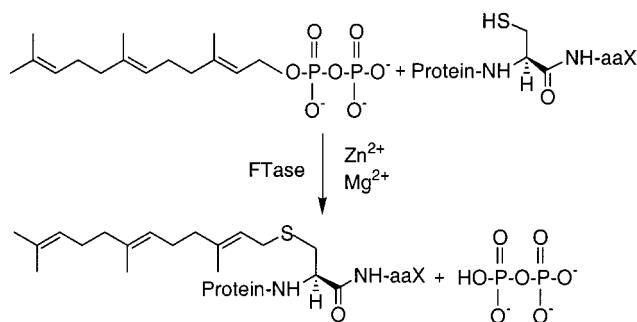
Department of Biochemistry, Box 3711, Duke University Medical Center, Durham, North Carolina 27710

Received May 24, 2000; Revised Manuscript Received August 2, 2000

ABSTRACT: Protein farnesyltransferase catalyzes the posttranslational farnesylation of several proteins involved in signal transduction, including Ras, and is a target enzyme for antitumor therapies. Efficient product formation catalyzed by protein farnesyltransferase requires an enzyme-bound zinc cation and high concentrations of magnesium ions. In this work, we have measured the pH dependence of the chemical step of product formation, determined under single-turnover conditions, and have demonstrated that the prenylation rate constant is enhanced by two deprotonations. Substitution of the active site zinc by cadmium demonstrated that one of the ionizations reflects deprotonation of the metal-coordinated thiol of the peptide “CaaX” motif, $pK_{a1} = 6.0$. These data provide additional evidence for the direct involvement of a metal-coordinated sulfur nucleophile in catalysis. The second ionization was assigned to a hydroxyl on the pyrophosphate moiety of farnesyl pyrophosphate, $pK_{a2} = 7.4$. Deprotonation of this group is important for binding of magnesium. This second ionization is not observed for catalysis in the absence of magnesium or when the substrate is farnesyl monophosphate. These data indicate that the maximal rate constant for prenylation requires formation of a zinc-coordinated thiolate nucleophile and enhancement of the electrophilic character at C1 of the farnesyl chain by magnesium ion coordination of the pyrophosphate leaving group.

Protein farnesyltransferase (FTase)¹ catalyzes the formation of a thioether linkage (Scheme 1) between the 15-carbon farnesyl group of farnesyl pyrophosphate (FPP) and the cysteine residue of the carboxyl-terminal “CaaX” motif of proteins such as Ras, nuclear lamins A and B, and several proteins involved in visual signal transduction (1, 2). Farnesylation of these proteins is essential for membrane integration and may facilitate protein–protein interactions (1, 3). The transformation of normal cells into cancerous cells by oncogenic forms of Ras is dependent upon membrane localization via the farnesyl group (4–6). Because Ras mutations have been implicated in up to 30% of all human cancers, inhibition of FTase is a potential target for antitumor therapies (7–9).

Scheme 1: Reaction Catalyzed by FTase



FTase is an α/β heterodimeric metalloenzyme that contains an active site zinc ion that is required for catalytic activity (10–12) and peptide/protein binding (10, 12). The zinc ion directly coordinates the sulfur atom of the “CaaX” cysteine residue (13, 14), thereby lowering the pK_a of the bound “CaaX” cysteine thiol so that the thiolate anion is present at physiological pH (15, 16). The metal-bound thiolate reacts with C1 of FPP in an associative reaction where the transition state contains a partial negative charge on the zinc-coordinated sulfur and a partial positive charge on C1 of FPP (12, 17). A zinc-coordinated nucleophile has been proposed as the general mechanism for the greater family of zinc metalloproteins that facilitate the transfer of an alkyl group to sulfur and selenium residues (18–20).

In addition to the tightly bound zinc, millimolar concentrations of magnesium ions are required for maximal levels of activity under both single-turnover and steady-state conditions (10, 12, 21). The role of magnesium ions in the reaction catalyzed by FTase is not well understood. Previous work has suggested that the magnesium facilitates a step or steps

[†] This work was supported by National Institutes of Health Grant GM40602 (C.A.F.) and the Cancer Research fund of the Damon Runyon–Walter Winchell Foundation Fellowship DRG-1450 (K.E.H.).

* To whom correspondence should be addressed.

[‡] Present address: Department of Chemistry, CPO 1996, Berea College, Berea, KY 40404.

[§] Present address: Department of Pharmacology and Cancer Biology, Box 3686, Duke University Medical Center, Durham, NC 27710.

^{||} Present address: Department of Chemistry, University of Michigan, 930 N. University, Ann Arbor, MI 48109-1055. Tel: (734) 936-2678. Fax: (734) 647-4865. E-mail: fierke@umich.edu.

¹ Abbreviations: FTase, protein farnesyltransferase; FPP, farnesyl pyrophosphate; apo-FTase, FTase without bound metal; Heppso, *N*-(2-hydroxyethyl)piperazine-*N'*-2-hydroxypropanesulfonic acid; TCEP, tris-(2-carboxyethyl)phosphine hydrochloride; Zn-FTase, FTase with bound Zn²⁺; Cd-FTase, FTase with bound Cd²⁺; Mes, 2-(*N*-morpholino)-ethanesulfonic acid; Bes, *N,N*-bis(2-hydroxyethyl)-2-aminoethanesulfonic acid; Bicine, *N,N*-bis(2-hydroxyethyl)glycine; [³H]FPP, tritium-labeled farnesyl pyrophosphate; GCVLS, pentapeptide Gly-Cys-Val-Leu-Ser; TLC, thin-layer chromatography; [³H]FMP, tritium-labeled farnesyl monophosphate; GGTase-I, protein geranylgeranyltransferase type I.

after formation of the ternary substrate complex (12). Magnesium coordination of the nonbridging oxygens of FPP has been proposed to polarize the pyrophosphate moiety and make it a better leaving group to facilitate formation of the positive charge at C1 (12). Metal-dependent activation of a pyrophosphate leaving group has also been proposed for solvolysis of prenyl pyrophosphates (22–25) and for enzymes involved in the synthesis of prenyl pyrophosphates (22, 26–28), terpenes (23, 27, 29), and nucleotides (30–32). However, in most of these cases, a conserved group of acidic amino acids have been identified as a magnesium binding site. A similar site has not been identified in FTase, although a recent crystal structure of an FTase ternary complex containing a K-Ras4B peptide and a FPP analogue positions a bound manganese ion in the vicinity of the pyrophosphate (33).

In this work, we further investigate the role of zinc and magnesium ions in the catalytic mechanism of FTase. The pH dependence of the chemical step of product formation reveals two ionizations that increase the rate constant for formation of the thioether product. One ionization is consistent with deprotonation of the bound peptide cysteine thiol to form a metal-coordinated thiolate that acts as a nucleophile in the reaction. The other ionization decreases the concentration of magnesium required to activate farnesylation (K_{Mg}), and additional evidence supports the assignment of this pK_a to a hydroxyl of the pyrophosphate moiety of FPP.

EXPERIMENTAL PROCEDURES

Preparation of FTase. Recombinant rat FTase was over-expressed in *Escherichia coli* and purified as described previously (34). The bound zinc ion was removed from FTase (apo-FTase) by dialysis against 50 mM Heppso–NaOH (pH 7.8), 1 mM tris(2-carboxyethyl)phosphine (TCEP), and 5 mM EDTA for 24 h followed by an additional 24 h against 50 mM Heppso–NaOH (pH 7.8), 1 mM TCEP, and 50 μ M EDTA. The apo-FTase was reconstituted with zinc (Zn-FTase) or cadmium (Cd-FTase) as described previously (12).

Transient Kinetics. Single-turnover assays were conducted between pH 4.8 and 9.0 using 50 mM buffer [Mes–NaOH (pH 4.8–6.0), Bis–NaOH (pH 6.0–7.0), Heppso–NaOH (pH 7.0–8.0), and Bicine–NaOH (pH 8.0–9.0)], with the ionic strength maintained at 0.1 M with NaCl, and 5 mM TCEP, with or without 5 mM $MgCl_2$. The enzyme is stable over this pH range (15), and the peptide concentration used in these assays was saturating at all pH values (data not shown). For observed rate constants for product formation slower than 0.1 s^{-1} , FTase was preincubated with tritium-labeled FPP ($[^3H]FPP$), and then the reaction was initiated by the addition of the peptide GCVLS so that the final concentrations were 0.8 μ M FTase, 0.4 μ M $[^3H]FPP$, and 100 μ M GCVLS (8 μ L total volume). The reactions were stopped at various times (5 s to 20 min) by the addition of 8 μ L of 2-propanol. A KinTek rapid quench apparatus was used for reactions where the observed rate constants of product formation were faster than 0.1 s^{-1} . These reactions were initiated by the addition of GCVLS to a FTase• $[^3H]$ -FPP binary complex so that the final concentrations were 0.2 μ M FTase, 0.1 μ M $[^3H]FPP$, and 100 μ M GCVLS (30 μ L total volume). The reactions were quenched at various

times (0.005–60 s) by the addition of 100 μ L of 20% acetic acid, 80% 2-propanol. The samples were dried under vacuum and resuspended in 12 μ L of 50% 2-propanol. Products were separated from substrates by thin-layer chromatography (TLC) on silica gel plates with an 8:1:1 (v/v/v) 2-propanol/ NH_4OH/H_2O mobile phase. Tritiated substrates and products were visualized by autoradiography with an intensifying screen (TranScreen-LE; Kodak, Rochester, NY) or following fluorographic enhancement (En³Hance; NEN LifeSciences, Boston, MA). The bands corresponding to substrates and products were excised, and the percentage product formed was calculated from the ratio of the radioactivity in the product band to the total radioactivity. The observed rate constants for product formation, k_{obs} , were calculated from a fit of the data to eq 1 (pH >5.5) or eq 2 (pH ≤5.5):

$$\frac{P_t}{P_\infty} = 1 - e^{-k_{obs}t} \quad (1)$$

$$\frac{P_t}{P_\infty} = A_1(1 - e^{-k_{1obs}t}) + A_2(1 - e^{-k_{2obs}t}) \quad (2)$$

where P_t is the product formed at time t , P_∞ is the endpoint of the reaction which ranged from 65% to 90%, and A_1 and A_2 are the amplitudes of each phase. For the low-pH reactions, the faster of the two rate constants was included in the pH rate profile.

The pK_a value(s) associated with the chemical step were calculated from the pH dependence of $\log(k_{obs})$ using weighted fits to the log form of eq 3 for reactions performed in the presence of magnesium and to the log form of eq 4 for reactions performed in the absence of magnesium:

$$k_{obs} = k_{max} / [1 + 10^{(pK_{a1}-pH)} + 10^{(pK_{a2}-pH)} + 10^{(pK_{a1}+pK_{a2}-2pH)}] \quad (3)$$

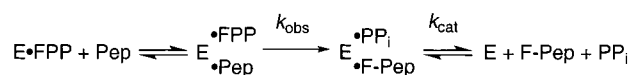
$$k_{obs} = \frac{k_{max}}{1 + 10^{(pK_{a1}-pH)}} \quad (4)$$

where k_{max} is the pH-independent maximal rate constant for product formation.

Magnesium Dependence of Product Formation. These reactions were performed essentially as described above except that the ionic strength was maintained, with the exception of the pH 5.5 reactions performed with 100 mM $MgCl_2$, at 0.114 M by decreasing the concentration of added NaCl as the concentration of $MgCl_2$ increased up to 38 mM. The observed rate constants for product formation, determined at varying pH (5.5–9.1) and magnesium concentrations (0–100 mM), were calculated using eqs 1 and 2. These rate constants were used to determine k_{max}^{Mg} , the calculated maximal rate constant for product formation at saturating magnesium concentrations at a given pH, and K_{Mg} , the apparent dissociation constant for magnesium at that pH, by fitting the data to eq 5:

$$k_{obs} = \frac{k_{max}^{Mg}}{1 + K_{Mg}/[Mg^{2+}]} + k_0 \quad (5)$$

where k_0 is the rate constant in the absence of magnesium. The k_{max}^{Mg} values, calculated from eq 5, were used to

Scheme 2: Kinetic Scheme for FTase^a

^a E = protein farnesyltransferase; FPP = farnesylpyrophosphate; Pep = peptide substrate; and F-Pep = farnesylated peptide product.

determine the pH dependence of product formation at saturating magnesium using a weighted fit to eq 4. The apparent pK_a of the group interacting with the magnesium ion was obtained from a weighted fit to eq 6:

$$K_{Mg}^{app} = K_{1/2}[1 + 10^{(pK_a - pH)}] \quad (6)$$

Reaction with FMP. Assays for the reaction of FTase with tritium-labeled farnesyl monophosphate ($[^3H]FMP$) were performed as described above for $[^3H]FPP$. Separation of substrates and products was accomplished by TLC using a 7:2:1 (v/v/v) 2-propanol/ NH_4OH/H_2O mobile phase. The individual observed rate constants for product formation were calculated using eq 1. The $\log(k_{obs})$ at varying pH were fit, with weighting, to the log form of an equation (eq 7) describing two ionizations:

$$k_{obs} = k_{max}/[1 + 10^{(pK_{a1} - pH)} + 10^{(pH - pK_{a2})} + 10^{(pK_{a1} - pK_{a2})}] \quad (7)$$

where k_{max} is the maximal rate constant for product formation.

Miscellaneous Methods. Protein concentrations were determined using the method of Bradford (35) and a commercially available dye (BioRad). The peptide substrate GCVLS ($\geq 95\%$ pure) was synthesized using manual solid-phase techniques and purified by HPLC. Peptide concentrations were determined from the reaction of the cysteine group with 5,5'-dithiobis(2-nitrobenzoic acid) (36) using an extinction coefficient of $14\,150\,M^{-1}cm^{-1}$ (37). $[^3H]FPP$ (20.5 Ci/mmol) was obtained from NEN LifeSciences (Boston, MA), and $[^3H]FMP$ (15 Ci/mmol) was obtained from American Radiolabeled Chemicals, Inc. (St. Louis, MO). All reactions were conducted at 25 °C, and curve fitting was performed with KaleidaGraph (Synergy Software).

RESULTS AND DISCUSSION

A basic kinetic scheme for the reaction catalyzed by FTase is shown in Scheme 2. For mammalian FTase, substrate binding and product release are rate-limiting for steady-state catalysis under conditions of subsaturating and saturating substrate concentrations, respectively (38, 39). Therefore, the steady-state kinetic parameters, k_{cat} and k_{cat}/K_M , do not necessarily provide information on the chemical step of the reaction. To study ionizations that enhance formation of the thioether product, it is necessary to isolate the chemical step. The chemical step can be isolated by performing single-turnover assays with limiting $[^3H]FPP$ (12) and high peptide concentrations (100 μM) so that formation of the ternary complex is fast relative to the rate constant for product formation and essentially irreversible (12, 14, 38). The assays are initiated by the addition of the peptide substrate to a preformed FTase· $[^3H]FPP$ binary complex. Under these conditions, the observed rate constant for product formation (chemistry), k_{obs} , can be determined. Single-turnover assays

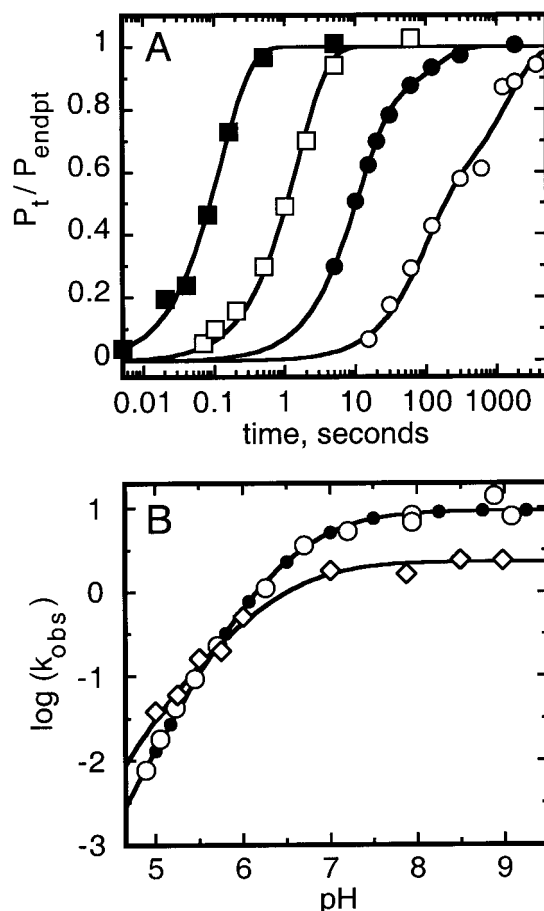


FIGURE 1: pH dependence of product formation. Single-turnover assays at various pH values (4.7–9.1) were conducted as described under Experimental Procedures. (A) Product formation with Zn-FTase at pH 4.7 (○), 5.5 (●), 6.2 (□), and 9.1 (■). A single-exponential equation (eq 1) is used to fit the data at pH 9.1 and 6.2, and a double-exponential equation (eq 2) is used to fit the lower pH values. (B) pH dependence of product formation by Zn-FTase (○) and Cd-FTase (◇) in 5 mM $MgCl_2$. The pK_a values associated with these data were calculated from eq 3 (see Table 1). The filled circles are calculated using eq 8, derived from the pH and magnesium dependence illustrated in Scheme 3 assuming that all of the protonation and magnesium binding reactions are rapid compared to alkylation, with the following values (taken from Figures 1 and 3): $k_{max} = 13\,s^{-1}$, $pK_{a1} = pK_{a2} = pK_{a3} = 6.0$, $pK_{a4} = pK_{a5} = 7.4$, and $K_{Mg1} = K_{Mg2} = 2\,mM$.

have previously been used to study the characteristics of the transition state of the reaction catalyzed by FTase (12).

pH Dependence of Product Formation. To investigate ionizations that enhance the observed rate constant for formation of the thioether product, the single-turnover rate constant, k_{obs} , was determined over a range of pH values (4.8–9.0). The individual reactions proceed to completion and are well-described by a single-exponential equation (eq 1) above pH 5.5 (Figure 1A). Below this pH, the reaction is biphasic with a rapid phase accounting for 50–90% of the reaction and a second phase with a rate constant that is more than 10-fold slower than the first phase. The rate constant of the first phase (eq 2) was used in the analysis of the pH dependence of this reaction. A plot of the pH dependence of $\log(k_{obs})$ for the reaction catalyzed by Zn-FTase in the presence of 5 mM $MgCl_2$ is shown in Figure 1B. At low pH, $\log(k_{obs})$ is linearly dependent upon pH with a slope of 2, indicating that the reaction is characterized by two

Table 1: pH Dependence of Product Formation

	Mg ²⁺ ^a	k_{\max} (s ⁻¹) ^b	pK _{a1}	pK _{a2} ^c
Zn-FTase	+	10 ± 1	6.0 ± 0.1	6.8 ± 0.1
Zn-FTase	-	0.015 ± 0.001	5.6 ± 0.2	ND
Cd-FTase	+	2.3 ± 0.1	5.0 ± 0.2	6.6 ± 0.1
Cd-FTase	-	0.010 ± 0.001	5.3 ± 0.1	ND

^a These assays were performed with (+) or without (-) 5 mM MgCl₂.

^b k_{\max} is the pH-independent maximum rate constant for product formation. ^c A second pK_a was not detected (ND) in the absence of magnesium.

ionizations (40). Fitting these data to the log of an equation describing two ionizations (eq 3) where either protonated species is inactive results in values of pK_{a1} = 6.0 ± 0.1 and pK_{a2} = 6.8 ± 0.1 (Table 1). The pH-independent maximal value of k_{obs} calculated from this fit, k_{\max} = 10 ± 1 s⁻¹, is in agreement with previously reported values for the rate constant for product formation at high pH (12, 14, 38). The pK_a values observed in the pH dependence of product formation could represent ionization(s) of the enzyme and/or the substrates since both substrates have potential ionizing groups. In addition, these ionizations could reflect substrate binding or the chemical step of product formation. However, we used near-saturating concentrations of peptide and enzyme at all pH values (data not shown) so the pK_a values reflect ionizations in the E•FPP•peptide ternary complex. Furthermore, since product formation is essentially irreversible (12, 14, 38), only ionizations affecting the chemical step, or, possibly, a conformational change after the formation of a ternary complex and before thiol alkylation, will be observed. Regardless of the identities of the ionizing groups, the maximal rate constant for product formation is obtained when both sites are deprotonated. To assign the pK_a values to specific ionizations, we performed metal substitution and magnesium dependence studies.

One of the roles of the bound zinc ion in FTase is to lower the pK_a of the peptide cysteine thiol so that the thiolate anion can contribute as a nucleophile in the reaction at physiological pH (12, 15, 16). Previous work has shown that the pK_a of the metal-coordinated thiol, derived from binding studies utilizing FPP analogues, is approximately 6.4 (15, 16). Since both of the pK_a values obtained from the pH dependence of product formation (6.0 and 6.8) are close to the pK_a derived from the binding studies, we investigated which ionization is dependent upon the characteristics of the metal at the zinc site. Cadmium is a more thiophilic metal than zinc and should, consequently, coordinate the reactive sulfur of the peptide cysteine with higher affinity (41). This increased interaction has previously been observed as an increased binding affinity and a decreased rate constant for product formation, suggesting that the metal-coordinated thiolate is directly involved in the catalytic mechanism (12). Furthermore, binding studies suggest that the pK_a of the peptide thiol bound to Cd-FTase decreases (K. E. Hightower and C. A. Fierke, unpublished data). If the protonation state of the metal-coordinated sulfur is important for the rate constant for product formation, the observed pK_a of the peptide thiol should decrease for the cadmium-substituted enzyme. Indeed, when we measured the pH dependence of the single-turnover rate constant in 5 mM MgCl₂ (Figure 1B), pK_{a1} is significantly lower for Cd-FTase (5.0 ± 0.2) compared to Zn-FTase (6.0 ± 0.1) while the values for pK_{a2} are virtually unchanged

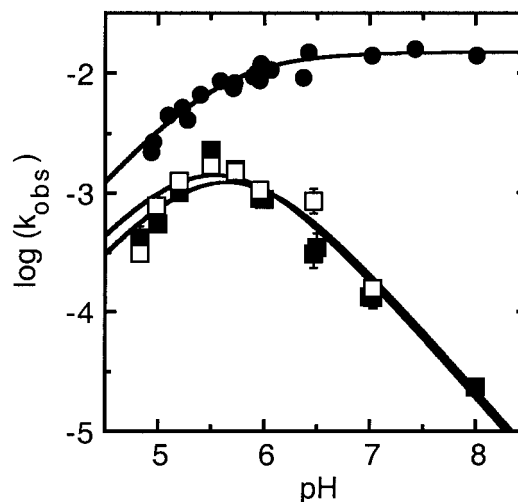


FIGURE 2: pH dependence of reaction using FPP or FMP substrates in the presence and absence of magnesium. The pH dependence of the reaction of Zn-FTase with FPP in the absence of magnesium (●) and FMP in the presence (□) and absence of magnesium (■) is shown. The pH dependence of k_{obs} for reaction of FPP with peptide, fit to eq 4, reveals a single pK_a with a value of 5.6 ± 0.2. Turnover of FMP is not dependent upon magnesium but is dependent upon two ionizations (eq 7) with pK_a values of approximately 5.5 (5.5 ± 0.7 and 5.5 ± 0.7).

(Table 1). The decrease of approximately 1 pH unit in pK_{a1} is consistent with the approximately 5-fold increase in peptide binding affinity for Cd-FTase relative to Zn-FTase (12). Thus, these data suggest that pK_{a1} describes the ionization of the metal-coordinated peptide thiol. Furthermore, in the single-turnover reactions the pH dependence is observed mainly as a decrease in k_{obs} (Figure 1A) rather than in the amplitude of the reaction, indicating that protonation/deprotonation is rapid compared to sulfur alkylation. The identity of the second ionization is discussed further in the next section.

Magnesium Dependence of FTase Activity. For FTase, we have previously demonstrated that magnesium is not required for formation of the thioether product but the presence of magnesium increases the single-turnover rate constant by several orders of magnitude at saturating enzyme and substrate concentrations (12). Therefore, magnesium is involved in a step following formation of the ternary complex and at or before chemistry. In the pH dependence of the single-turnover reaction in the absence of magnesium, only a single ionization is observed with a pK_a value of 5.6 ± 0.2 and a maximal value of k_{obs} of 0.015 s⁻¹ (Figure 2; Table 1). Although this pK_a is presumed to reflect ionization of the bound peptide thiol, the cadmium effect is not observed under these conditions (Table 1), consistent with previous results (12). The absence of a second ionization in the absence of magnesium suggests that pK_{a2} is involved in magnesium binding or reactivity.

To further test this hypothesis, we determined the magnesium dependence of the single-turnover reaction at various pH values. As shown in Figure 3A, the rate constant for the reaction catalyzed by FTase is enhanced by the addition of magnesium throughout the pH range studied. From these data, the apparent dissociation constant for magnesium, K_{Mg} , and the maximal rate constant for product formation at saturating concentrations of magnesium, k_{\max}^{Mg} , can be

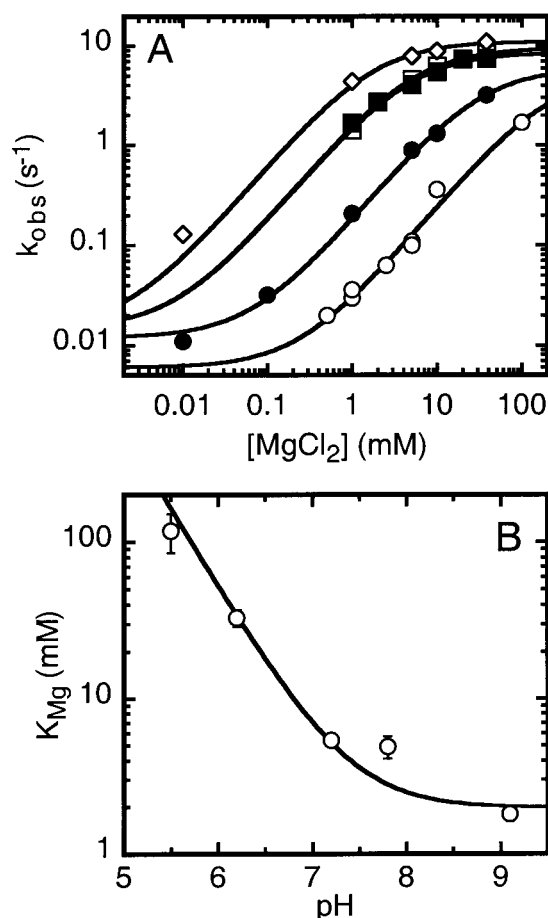
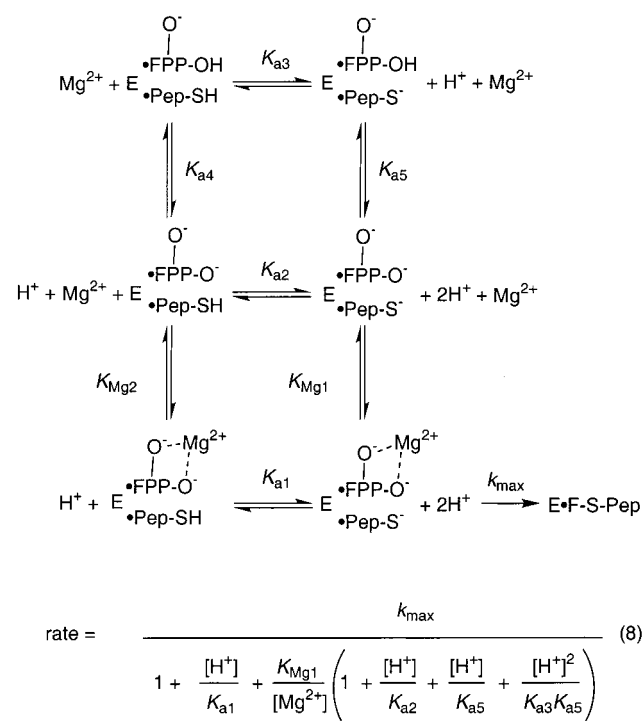


FIGURE 3: Influence of magnesium on single-turnover reactions catalyzed by FTase. (A) The observed rate constants for product formation were determined at varying pH (5.5–9.1) and magnesium concentration (0–100 mM) with Zn-FTase as described under Experimental Procedures. The plot shows the magnesium dependence of Zn-FTase activity at pH 5.5 (○), 6.2 (●), 7.2 (□), 7.8 (■), and 9.1 (◇). The data are fit using eq 5. (B) The pH dependence of the apparent magnesium dissociation constant, K_{Mg} , indicates that the group coordinating the magnesium has a $\text{p}K_{\text{a}}$ of 7.4 ± 0.1 and that the pH-independent $K_{1/2}$ for magnesium is 2.0 ± 0.2 mM (eq 6).

estimated. A plot of the pH dependence of K_{Mg} (Figure 3B) demonstrates that this parameter increases as the pH is lowered and can be described by a single ionization with a $\text{p}K_{\text{a}}$ value of 7.4 ± 0.1 . The $\text{p}K_{\text{a}}$ reflects the ionization of a group that enhances the apparent affinity of magnesium. This value is slightly higher than the previously determined value of 6.8 ± 0.2 for $\text{p}K_{\text{a}2}$ at 5 mM MgCl_2 (Figure 1B), as expected since the apparent $\text{p}K_{\text{a}}$ is magnesium dependent (see Scheme 3). Furthermore, the $K_{1/2}$ for magnesium, 2.0 ± 0.2 mM, is consistent with previous reports of the magnesium requirement for steady-state catalysis by FTase (10, 21, 42, 43) and for several other enzymes where magnesium has been proposed to play a role in activation of a pyrophosphate leaving group (28, 29, 31, 32). Additionally, the value of $k_{\text{max}}^{\text{Mg}}$ decreases about 3-fold as the pH is lowered from 9 to 5.5. This decrease in activity could reflect an ionization with a $\text{p}K_{\text{a}}$ near 6, consistent with the value of $\text{p}K_{\text{a}1}$ calculated from the pH dependence of the reaction at 5 mM MgCl_2 (Figure 1B) and with the previously reported $\text{p}K_{\text{a}}$ value of the bound cysteine thiol from peptide binding studies (15, 16). Therefore, this modest decrease in activity

Scheme 3: Model for the pH Dependence of FTase Activity



could reflect ionization of the peptide thiol in the $\text{E} \cdot \text{FPP} \cdot \text{Mg} \cdot \text{peptide}$ complex.

One proposed catalytic role for the magnesium ion is coordination of the nonbridging pyrophosphate oxygens of FPP to stabilize the pyrophosphate leaving group, as observed in other enzymes (22, 26–30). For pyrophosphate, the tetrabasic species binds magnesium with the highest affinity ($K_{\text{Mg}} = 20 \mu\text{M}$) with protonation decreasing affinity (44). Similarly, magnesium coordination by alkyl pyrophosphates should be pH-dependent, suggesting that the $\text{p}K_{\text{a}}$ observed in the pH dependence of K_{Mg} could reflect ionization of bound FPP. Previous work on the hydrolysis of alkyl phosphates and alkyl pyrophosphates has established $\text{p}K_{\text{a}}$ values of approximately 1, 2–3, and 6.2–8 (24, 45) for the hydroxyl groups, which are consistent with the $\text{p}K_{\text{a}}$ values for pyrophosphate (46–49). Furthermore, the highest $\text{p}K_{\text{a}}$ is consistent with the value of $\text{p}K_{\text{a}2}$. While it is not possible to rule out ionization of a group on the enzyme from these data, the assignment of $\text{p}K_{\text{a}2}$ to a FPP hydroxyl is consistent with the data presented here.

Product Formation with FMP. To test the proposal that $\text{p}K_{\text{a}2}$ reflects ionization of enzyme-bound FPP and to further investigate the substrate specificity of FTase, we examined whether farnesyl monophosphate (FMP) is a substrate for this enzyme. Under single-turnover conditions, FTase catalyzes the reaction of FMP with GCVLS to form a product that has the same migration on TLC plates as the farnesyl-peptide product of the reaction with FPP. However, k_{max} for product formation with FMP is decreased substantially ($0.005\text{--}0.006 \text{ s}^{-1}$, Figure 2), comparable to k_{max} for FPP in the absence of magnesium (0.015 s^{-1}). Significantly, the reaction with FMP is not enhanced by the addition of MgCl_2 , consistent with the pyrophosphate moiety of FPP coordinating Mg^{2+} since the magnesium affinity of the monophosphate moiety is decreased substantially (23). Additionally, the pH dependence of the single-turnover rate constant for farnesyl-

sylation using FMP is significantly altered (Figure 2); the pH dependence is described by a bell-shaped curve indicating that two ionizations, one protonation and one deprotonation, are important for catalysis. The apparent pK_a values associated with these ionizations are both approximately 5.5, in either the presence or the absence of magnesium (Figure 2). The decreased activity at low pH can most reasonably be attributed to protonation of the zinc-bound peptide thiolate which decreases the concentration of the nucleophilic thiolate and, consequently, lowers the observed rate constant for product formation. The FTase-catalyzed farnesylation of peptides using FMP as a substrate is not activated by either magnesium or a second deprotonation. This result is consistent with the hypothesis that pK_{a2} observed for FPP reflects deprotonation of the pyrophosphate moiety of FPP. On the contrary, for FMP the rate decreases at higher pH. One chemically reasonable mechanism for this observed pH dependence is that protonation of the phosphate leaving group at low pH increases the reactivity by stabilizing product formation in the transition state. At higher pH, the phosphate group of FMP ionizes [$R-OPO_3H^- \leftrightarrow R-OPO_3^{2-} + H^+$; $pK_a \sim 6-7$ in solution (24, 45)], decreasing the stability of the phosphate leaving group and decreasing the observed rate constant for product formation. A similar pH dependence has been observed for hydrolysis of alkyl phosphates in solution (45). Although we have not definitively demonstrated that this ionization cannot be attributed to a side chain group, the drastic differences in the pH dependence of FPP and FMP suggest that ionization of the leaving group is more likely.

Models of pH Dependence. Together, the findings presented here support the assignment of pK_{a1} to the metal-coordinated peptide cysteine thiol and pK_{a2} to a pyrophosphate hydroxyl group. A model for the pH dependence of product formation is shown in Scheme 3. In the presence of saturating magnesium, the maximal rate constant for product formation, k_{max} , is achieved when both sites are deprotonated: the thiol is ionized to the thiolate to act as a nucleophile, and the pyrophosphate hydroxyl is ionized to enhance magnesium coordination. From this scheme, an equation (eq 8, Scheme 3) describing the pH and magnesium dependence can be derived assuming that all of the protonation and magnesium binding reactions are rapid compared to alkylation. The observed pH dependence at 5 mM magnesium (Figure 1B) is adequately described by this model, with the added simplification that the two ionizations are independent, using the following values taken from Figures 1B and 3B: $pK_{a1} = pK_{a2} = pK_{a3} = 6.0$, $pK_{a4} = pK_{a5} = 7.4$, and $K_{Mg1} = K_{Mg2} = 2$ mM. In the absence of magnesium, product formation is dependent upon formation of the metal-bound thiolate but not upon ionization of the pyrophosphate hydroxyl. This model adequately describes the pH dependence of substrate binding and single-turnover kinetics. If these were the only ionizations important for catalytic turnover, the pH dependence of the steady-state kinetic parameters (k_{cat} and k_{cat}/K_M) should show behavior similar to the single-turnover data. However, the pK_a values would be kinetically perturbed due to the slow rate constant for dissociation of substrates and product compared to the alkylation rate constant (12, 14, 38, 39, 50). Consistent with our data, a recent determination of the steady-state pH–rate profiles of wild-type FTase (17) reveals two acidic titratable

groups with pK_a values of 6 and 7, although one of these ionizations is not observable in $V_{max}/K_M^{peptide}$, perhaps due to kinetic perturbation of the pK_a . Surprisingly, a third titratable group, with a basic pK_a of ~ 9 , was also observed in all the steady-state kinetic parameters except $V_{max}^{peptide}$. In our transient kinetic data, a decrease in activity at high pH was not observed for the reaction of the peptide GCVLS and FPP catalyzed by FTase. Potentially, the high pK_a observed in the steady-state kinetics could reflect ionization of a group that influences the rate constant for dissociation of substrates and/or products. Alternatively, this pK_a could reflect a new ionizable group that is introduced in the steady-state kinetic experiments, such as a lysine in the KKSKT-KCVIM substrate, a histidine in the His-tagged-FTase, or dithiothreitol in the buffer which is a substrate for FTase (K. E. Hightower and C. A. Fierke, unpublished data).

Implications for the Catalytic Mechanism. Much effort has been made to understand the catalytic mechanism of FTase driven, in part, by the desire to design new inhibitors as antitumor compounds. Early work established the requirement for zinc and magnesium in catalysis (10, 11, 21), the specificity of the enzyme for isoprenoid and protein/peptide substrates (10, 11, 51–58), and the general kinetic scheme for the reaction (38, 54, 59, 60). More recent work has focused on structure/function studies and in-depth investigations of the catalytic mechanism. This work has led to a proposed “exploded” associative transition state with a partial positive charge on C1, the reactive carbon of FPP, and a partial negative charge on the zinc-coordinated sulfur of the carboxyl-terminal “CaaX” motif cysteine (12, 17).

The role of the bound zinc ion in the reaction catalyzed by FTase has been well studied. The zinc is tightly bound to the enzyme and is required for catalysis and peptide/protein binding (10–12). The open coordination sphere of the zinc (61) and the direct coordination of the peptide cysteine thiol(ate) with the metal (12, 13) indicate that the zinc ion is directly involved in the catalytic mechanism. The decrease in the pK_a of the peptide cysteine thiol upon coordination with the metal suggests that the role of the zinc is to lower the pK_a of the thiol to maximize the amount of thiolate present at physiological pH while maintaining a relatively weak metal–sulfur bond (15, 16). Furthermore, metal-substitution studies have shown that the metal-coordinated thiolate is directly involved in the transition state of the reaction (12). The pH dependence of the rate constant for product formation catalyzed by Zn- and Cd-FTase described here indicates that the coordination of the metal with the sulfur lowers the pK_a of the peptide cysteine thiol and that this ionization is essential for the catalytic activity of the enzyme. These data provide more evidence for a metal-coordinated nucleophilic contribution to an associative transition state.

The role of magnesium in the reaction catalyzed by FTase has not been clearly established. Early work suggested that magnesium is necessary for steady-state catalysis (10, 21). However, the requirement for millimolar concentrations of magnesium for optimal activity indicates that the magnesium is not tightly associated with the enzyme. In addition, recent work has shown that magnesium does not enhance binding of either FPP or peptide in a binary E·S complex nor is it essential for the chemical step of product formation, although the presence of magnesium increases the rate constant for

product formation by several orders of magnitude (12). As described here, the magnesium dependence of product formation and the assignment of pK_{a2} to a pyrophosphate hydroxyl are consistent with the suggestion that the magnesium is coordinated by the pyrophosphate moiety of FPP. However, the apparent affinity of the enzyme-bound FPP for magnesium, $K_{1/2} = 2$ mM, is somewhat weaker than predicted from the magnesium affinity of nucleoside diphosphate compounds ($K_{Mg} \sim 0.2\text{--}0.7$ mM at high pH). Additionally, since magnesium does not enhance FPP binding (12), the magnesium affinity of enzyme-bound FPP and free FPP must be identical. This weaker than predicted affinity can be most easily rationalized by a decrease in the magnesium affinity of FPP upon formation of an E•FPP•peptide ternary complex, which has not yet been investigated. Consistent with this, previous studies have demonstrated synergy between the binding of peptide and FPP analogues to FTase (15). Alternatively, more than one magnesium may chelate FPP in the active site.

One possible role for magnesium in the reaction catalyzed by FTase is to activate the pyrophosphate leaving group. For FTase, activation of the leaving group could entail polarization of the pyrophosphate to facilitate formation of a positive charge on C1 of the farnesyl group and stabilization of the developing negative charge on the pyrophosphate in the transition state. Evidence for an electrophilic contribution to the transition state has been obtained from the decrease in the rate constant for product formation when electron-withdrawing fluorines are substituted at the C3 methyl position of FPP (12, 62).

The crystal structures of a FTase•FPP binary complex (63) and two FTase•isoprenoid•peptide ternary complexes (13, 33) suggest that the α -phosphate oxygens interact with Lys164 α and Arg291 β while the β -phosphate oxygens interact with His248 β , Arg291 β , Lys294 β , and Tyr300 β . Some of these residues, Arg291 β and Lys294 β in particular, have previously been implicated in FPP binding by mutational studies (64). The crystal structure of a ternary complex with bound manganese (33) shows that some of the positively charged residues, especially Lys164 α , may be displaced by coordination of the metal to the pyrophosphate. Decreases in the acidic pK_a in the steady-state pH–rate profiles for mutants at Lys164 α and Tyr300 β have led to the proposal that these groups may function as general acid/base catalysts (17). Our data suggest that the steady-state acidic pK_a values may reflect ionization of the metal-coordinated peptide cysteine thiol and a pyrophosphate hydroxyl group linked to magnesium binding (Scheme 3). A reasonable hypothesis for these altered pK_a values is that mutations near the pyrophosphate binding site affect ionization of the bound pyrophosphate moiety or the magnesium affinity. On the other hand, the altered pK_a values may simply reflect changes in the substrate and product “stickiness” (50) rather than alterations in the intrinsic ionizations.

Of some interest is a comparison of the roles of zinc and magnesium in the reactions catalyzed by FTase and the related enzyme protein geranylgeranyltransferase type I (GGTase-I). The metal polyhedron of the zinc site is preserved in these enzymes (18, 65), and it is likely that the zinc performs a similar function, coordinating to and lowering the pK_a of the “CaaX” motif cysteine thiol. However, the steady-state reaction of GGTase-I is not

dependent upon the presence of magnesium (42). This may suggest a fundamental difference in the catalytic mechanisms of these enzymes where a residue from the enzyme substitutes for the magnesium in the reaction catalyzed by GGTase-I. Additional work will be required to pinpoint the mechanistic differences between these two related prenyltransferases.

ACKNOWLEDGMENT

We thank Dr. Bruce W. Erickson (1942–1998) for the use of his laboratory for the peptide synthesis, Dr. Chih-chin Huang for assistance and helpful discussions, and Dr. Patrick Casey for encouragement and insightful comments.

REFERENCES

1. Zhang, F. L., and Casey, P. J. (1996) *Annu. Rev. Biochem.* 65, 241–269.
2. Casey, P. J., and Seabra, M. C. (1996) *J. Biol. Chem.* 271, 5289–5292.
3. Schafer, W. R., and Rine, J. (1992) *Annu. Rev. Genet.* 26, 209–237.
4. Hancock, J. F., Magee, A. I., Childs, J. E., and Marshall, C. J. (1989) *Cell* 57, 1167–1177.
5. Schafer, W. R., Kim, R., Sterne, R., Thorner, J., Kim, S. H., and Rine, J. (1989) *Science* 245, 379–385.
6. Casey, P. J., Solski, P. A., Der, C. J., and Buss, J. E. (1989) *Proc. Natl. Acad. Sci. U.S.A.* 86, 8323–8327.
7. Qian, Y., Sebt, S. M., and Hamilton, A. D. (1997) *Biopolymers* 43, 25–41.
8. Gibbs, J. B., and Oliff, A. (1997) *Annu. Rev. Pharmacol. Toxicol.* 37, 143–166.
9. Oliff, A. (1999) *Biochim. Biophys. Acta* 1423, C19–C30.
10. Reiss, Y., Brown, M. S., and Goldstein, J. L. (1992) *J. Biol. Chem.* 267, 6403–6408.
11. Chen, W. J., Moomaw, J. F., Overton, L., Kost, T. A., and Casey, P. J. (1993) *J. Biol. Chem.* 268, 9675–9680.
12. Huang, C., Hightower, K. E., and Fierke, C. A. (2000) *Biochemistry* 39, 2593–2602.
13. Strickland, C. L., Windsor, W. T., Syto, R., Wang, L., Bond, R., Wu, Z., Schwartz, J., Le, H. V., Beese, L. S., and Weber, P. C. (1998) *Biochemistry* 37, 16601–16611.
14. Huang, C., Casey, P. J., and Fierke, C. A. (1997) *J. Biol. Chem.* 272, 20–23.
15. Hightower, K. E., Huang, C., Casey, P. J., and Fierke, C. A. (1998) *Biochemistry* 37, 15555–15562.
16. Rozema, D. B., and Poulter, C. D. (1999) *Biochemistry* 38, 13138–13146.
17. Wu, Z., Demma, M., Strickland, C. L., Radisky, E. S., Poulter, C. D., Le, H. V., and Windsor, W. T. (1999) *Biochemistry* 38, 11239–11249.
18. Hightower, K. E., and Fierke, C. A. (1999) *Curr. Opin. Chem. Biol.* 3, 176–181.
19. Matthews, R. G., and Goulding, C. W. (1997) *Curr. Opin. Chem. Biol.* 1, 332–339.
20. Neuhierl, B., Thanbichler, M., Lottspeich, F., and Bock, A. (1999) *J. Biol. Chem.* 274, 5407–5414.
21. Moomaw, J. F., and Casey, P. J. (1992) *J. Biol. Chem.* 267, 17438–17443.
22. Brems, D. N., and Rilling, H. C. (1977) *J. Am. Chem. Soc.* 99, 8351–8352.
23. Vial, M. V., Portilla, G., Chayet, L., Pérez, M., Cori, O., and Bunton, C. A. (1981) *Tetrahedron* 37, 2351–2357.
24. Brody, E. P., and Gutsche, C. D. (1977) *Tetrahedron* 33, 723–729.
25. Chayet, L., Rojas, M. C., Cori, O., Bunton, C. A., and McKenzie, D. C. (1984) *Bioorg. Chem.* 12, 329–338.
26. Gotoh, T., Koyama, T., and Ogura, K. (2000) *Biochem. Biophys. Res. Commun.* 156, 396–402.
27. Wendt, K. U., and Schulz, G. E. (1998) *Structure* 6, 127–133.
28. Rojas, M. C., Chayet, L., Portilla, G., and Cori, O. (1983) *Arch. Biochem. Biophys.* 222, 389–396.

29. Pichersky, E., Lewinsohn, E., and Croteau, R. (1995) *Arch. Biochem. Biophys.* 316, 803–807.
30. Héroux, A., White, E. L., Ross, L. J., Davis, R. L., and Borhani, D. W. (2000) *Biochemistry* 38, 14495–14506.
31. Bhatia, M. B., and Grubmeyer, C. (2000) *Arch. Biochem. Biophys.* 303, 321–325.
32. Gadd, R. E. A., and Henderson, J. F. (1970) *Can. J. Biochem.* 48, 302–307.
33. Long, S. B., Casey, P. J., and Beese, L. S. (2000) *Structure* 8, 209–222.
34. Zimmerman, K. K., Scholten, J. D., Huang, C., Fierke, C. A., and Hupe, D. J. (1998) *Protein Express. Purif.* 14, 395–402.
35. Bradford, M. M. (1976) *Anal. Biochem.* 72, 248–254.
36. Ellman, G. L. (1959) *Arch. Biochem. Biophys.* 82, 70–77.
37. Riddles, P. W., Blakeley, R. L., and Zerner, B. (1979) *Anal. Biochem.* 94, 75–81.
38. Furfine, E. S., Leban, J. J., Landavazo, A., Moomaw, J. F., and Casey, P. J. (1995) *Biochemistry* 34, 6857–6862.
39. Tschantz, W. R., Furfine, E. S., and Casey, P. J. (1997) *J. Biol. Chem.* 272, 9989–9993.
40. Segel, I. H. (1975) *Enzyme Kinetics*, pp 896–898, John Wiley and Sons, New York.
41. Pearson, R. G. (1963) *J. Am. Chem. Soc.* 85, 3533–3539.
42. Zhang, F. L., and Casey, P. J. (1996) *Biochem. J.* 320, 925–932.
43. Manne, V., Roberts, D., Tobin, A., O'Rourke, E., DeVirgilio, M., Meyers, C., Ahmed, N., Kurz, B., Resh, M., Kung, H.-F., and Barbacid, M. (1990) *Proc. Natl. Acad. Sci. U.S.A.* 87, 7541–7545.
44. Dawson, R. M. E., Elliott, W. H., and Jones, K. M. (1986) *Data for Biochemical Research*, p 408, Clarendon Press, Oxford.
45. Tidd, B. K. (1971) *J. Am. Chem. Soc. (B)*, 1168–1176.
46. Delannoy, A., Hennion, J., Bavay, J.-C., and Nicole, J. (1979) *C. R. Hebd. Seances Acad. Sci., Ser. C* 289, 401–404.
47. Lambert, S. M., and Watters, J. I. (1957) *J. Am. Chem. Soc.* 79, 4262–4265.
48. Irani, R. R. (1961) *J. Phys. Chem.* 65, 1463–1465.
49. Frey, C. M., and Stuehr, J. E. (1972) *J. Am. Chem. Soc.* 94, 8898–8904.
50. Cleland, W. W. (1982) *Methods Enzymol.* 87, 390–405.
51. Yokoyama, K., Zimmerman, K., Scholten, J., and Gelb, M. H. (1997) *J. Biol. Chem.* 272, 3944–3952.
52. Reiss, Y., Goldstein, J. L., Seabra, M. C., Casey, P. J., and Brown, M. S. (1990) *Cell* 62, 81–88.
53. Trueblood, C. E., Boyartchuk, V. L., and Rine, J. (1997) *Proc. Natl. Acad. Sci. U.S.A.* 94, 10774–10779.
54. Pompliano, D. L., Schaber, M. D., Mosser, S. D., Omer, C. A., Shafer, J. A., and Gibbs, J. B. (1993) *Biochemistry* 32, 8341–8347.
55. Reiss, Y., Stradley, S. J., Gierasch, L. M., Brown, M. S., and Goldstein, J. L. (1991) *Proc. Natl. Acad. Sci. U.S.A.* 88, 732–736.
56. Brown, M. S., Goldstein, J. L., Paris, K. J., Burnier, J. P., and Marsters, J. C., Jr. (1992) *Proc. Natl. Acad. Sci. U.S.A.* 89, 8313–8316.
57. Omer, C. A., Kral, A. M., Diehl, R. E., Prendergast, G. C., Powers, S., Allen, C. M., Gibbs, J. B., and Kohl, N. E. (1993) *Biochemistry* 32, 5167–5176.
58. Goldstein, J. L., Brown, M. S., Stradley, S. J., Reiss, Y., and Gierasch, L. M. (1991) *J. Biol. Chem.* 266, 15575–15578.
59. Pompliano, D. L., Rands, E., Schaber, M. D., Mosser, S. D., Anthony, N. J., and Gibbs, J. B. (1992) *Biochemistry* 31, 3800–3807.
60. Dolence, J. M., Cassidy, P. B., Mathis, J. R., and Poulter, C. D. (1995) *Biochemistry* 34, 16687–16694.
61. Park, H. W., Boduluri, S. R., Moomaw, J. F., Casey, P. J., and Beese, L. S. (1997) *Science* 275, 1800–1804.
62. Dolence, J. M., and Poulter, C. D. (1995) *Proc. Natl. Acad. Sci. U.S.A.* 92, 5008–5011.
63. Long, S. B., Casey, P. J., and Beese, L. S. (1998) *Biochemistry* 37, 9612–9618.
64. Kral, A. M., Diehl, R. E., deSolms, S. J., Williams, T. M., Kohl, N. E., and Omer, C. A. (1997) *J. Biol. Chem.* 272, 27319–27323.
65. Zhang, F. L., Diehl, R. E., Kohl, N. E., Gibbs, J. B., Giros, B., Casey, P. J., and Omer, C. A. (1994) *J. Biol. Chem.* 269, 3175–3180.

BI0011781